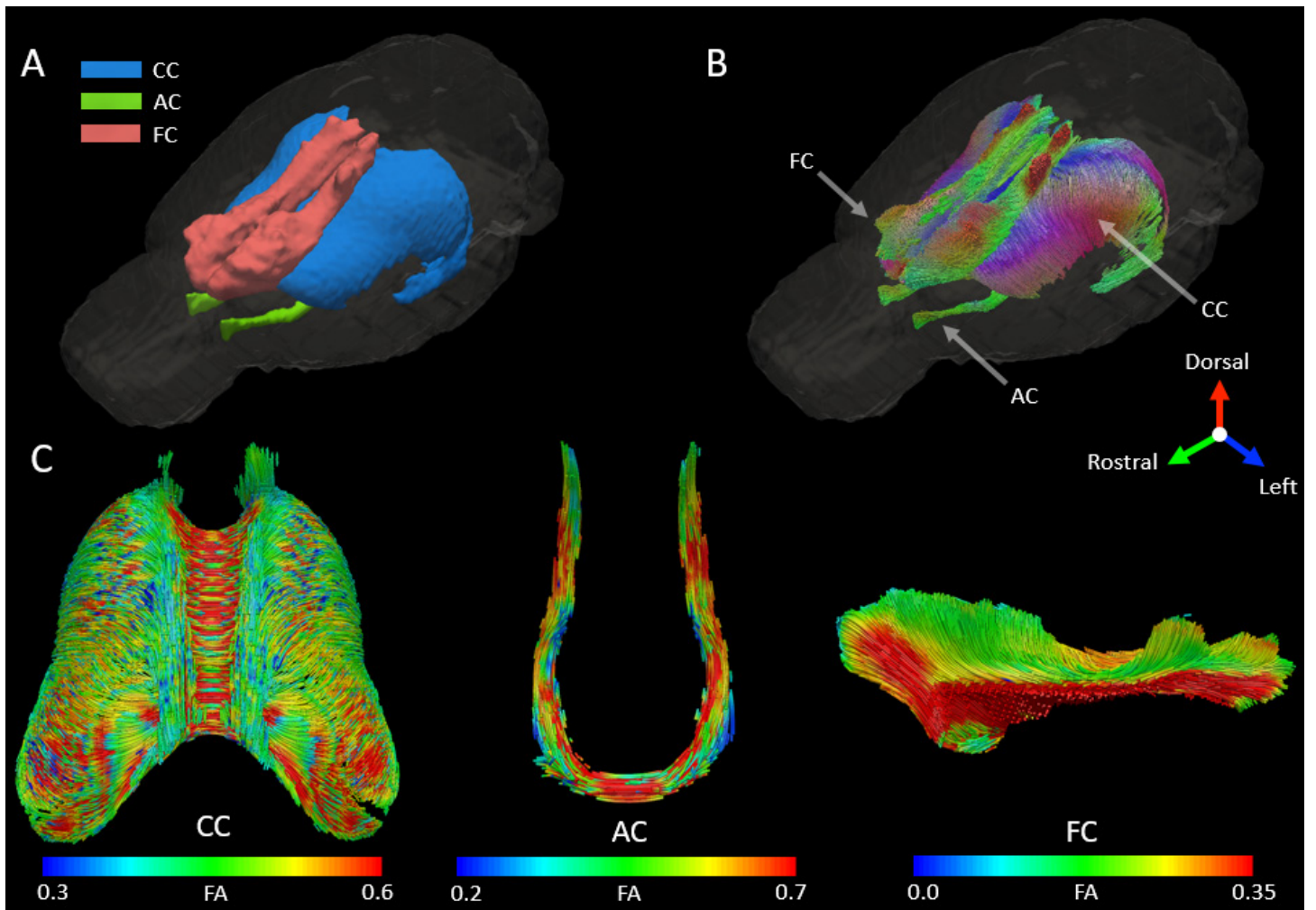


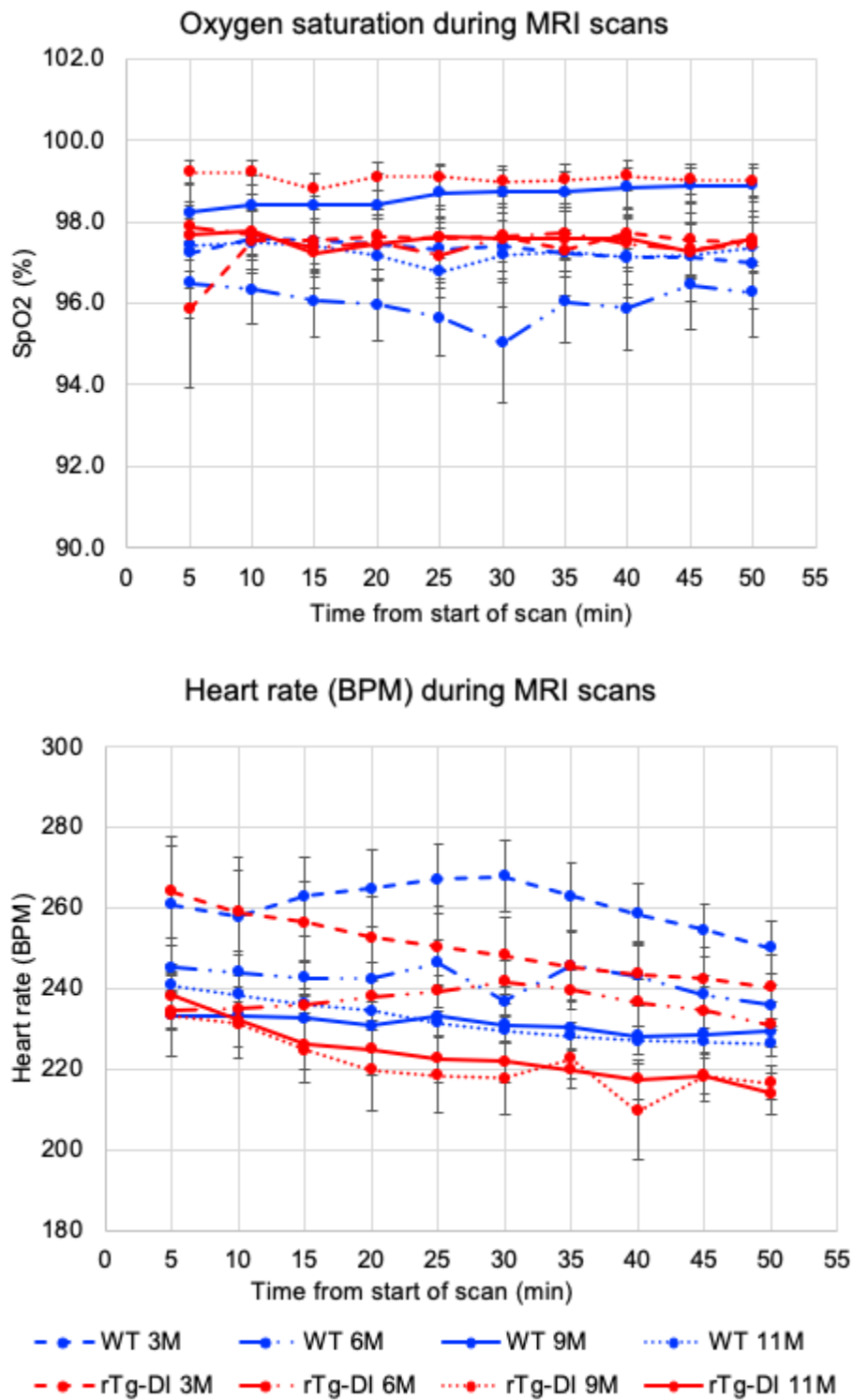
**Supplementary Figure 1: Population averaged proton density weighted images and tissue probability maps**

Voxel-based morphometry (VBM) was performed using custom made rTg-DI tissue probability maps (tpms). A total of 54 proton density weighted (PDW) scans (11 WT and 10 rTg-DI acquired at 4 time points) without conspicuous microbleeds were segmented, registered and population averaged using the unified segmentation method and DARTEL registration algorithm. The initial rTg-DI tpms were constructed by segmenting the PDW images using the publicly available Wistar tpms followed by manual editing to improve the accuracy as described in (Koundal et.al 2019).

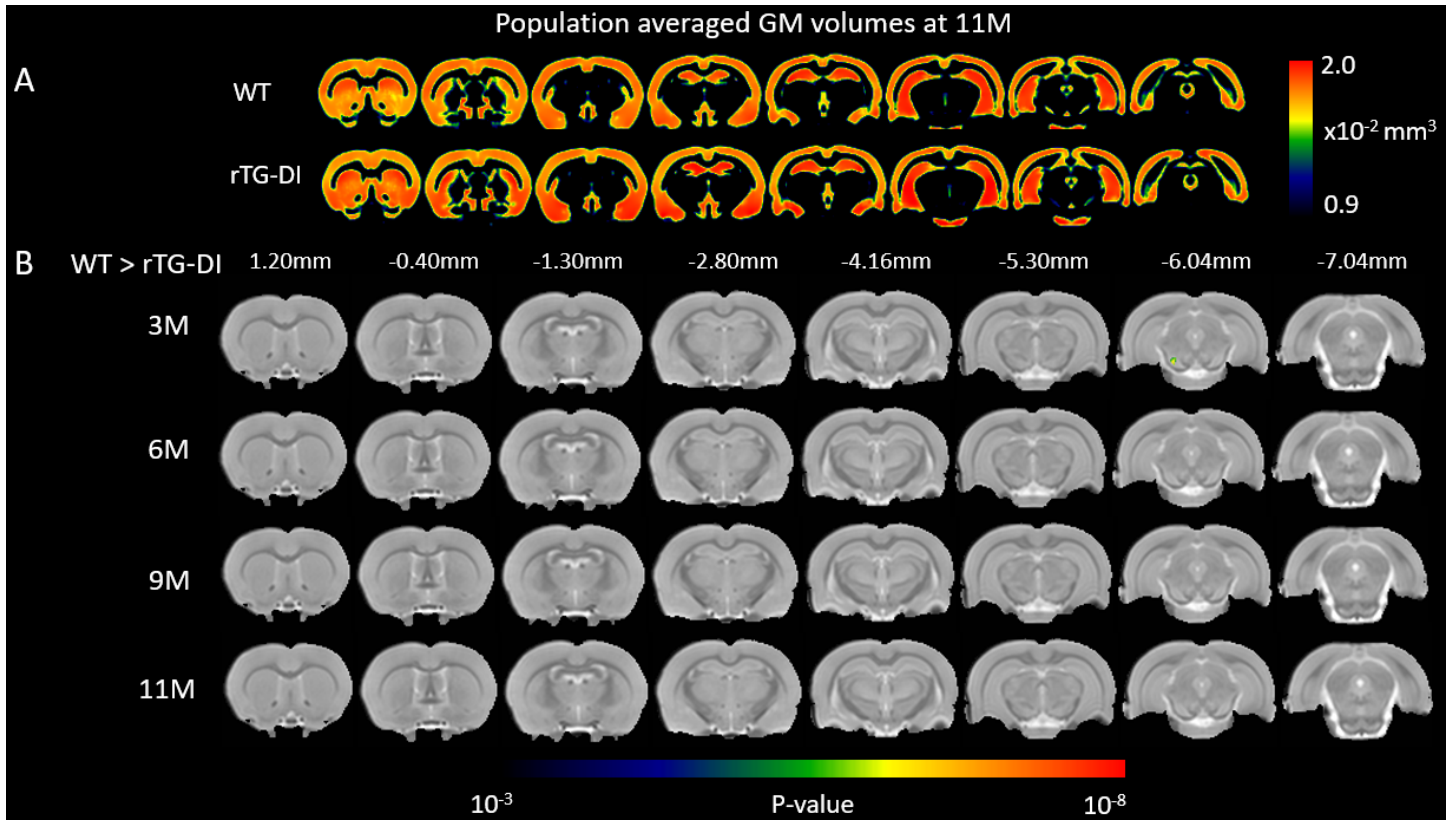


### Supplementary Figure 2: Delineation of regions of interest using tractography

**A:** Tractography guided manual delineation of corpus callosum (CC), anterior commissure (AC), and frontal cortex (FC) are shown. **B:** Streamlines represent population averaged and direction encoded fiber tracts within each region of interest (ROI). The arrows indicate the direction of color encoding. **C:** Streamlines represent population averaged and FA weighted fiber tracts within each region of interest (ROI).

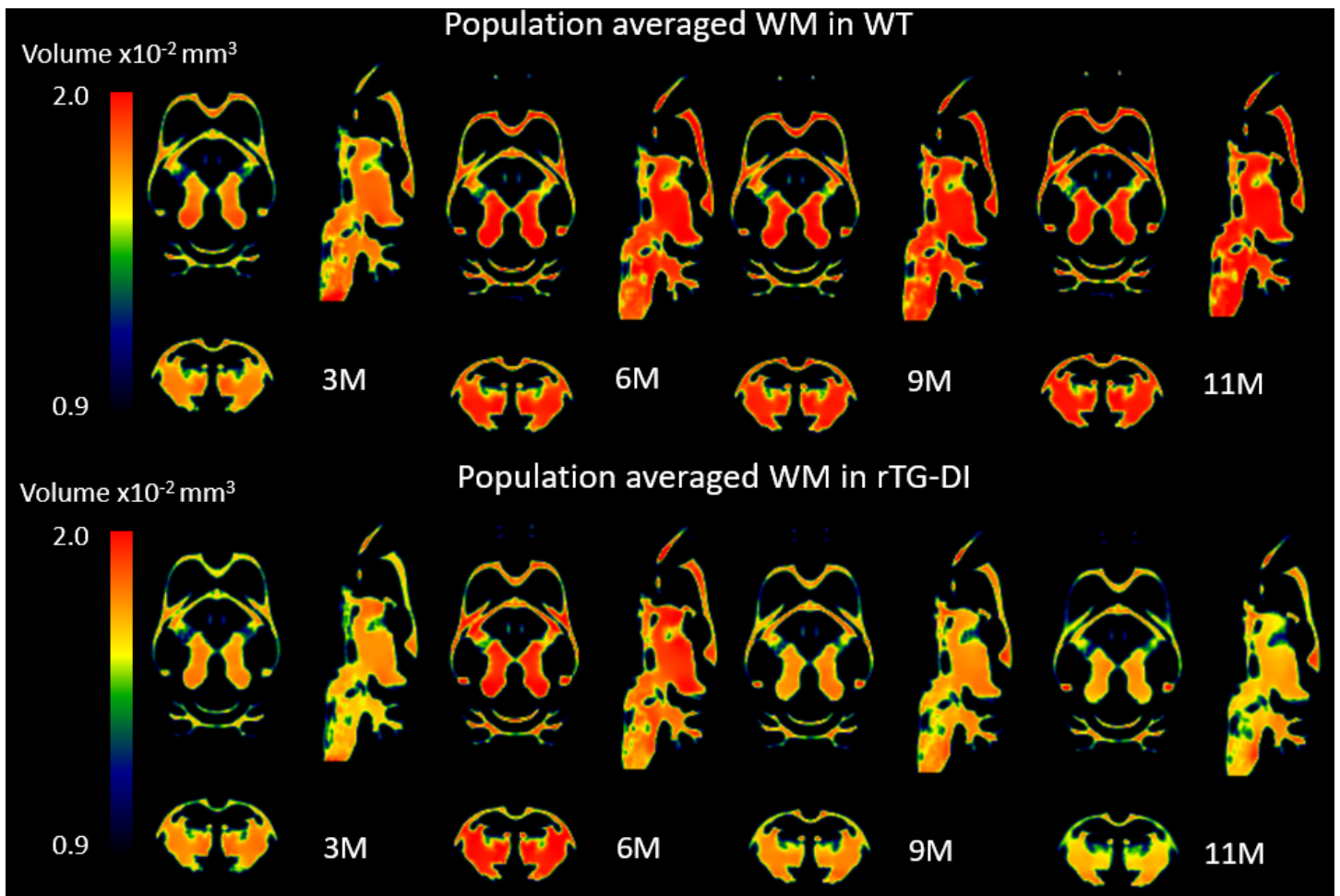


**Supplementary Figure 3: Blood oxygen saturation (top) and heart rate (bottom) parameters measured continuously in the rats during the four different MRI scanning sessions.**



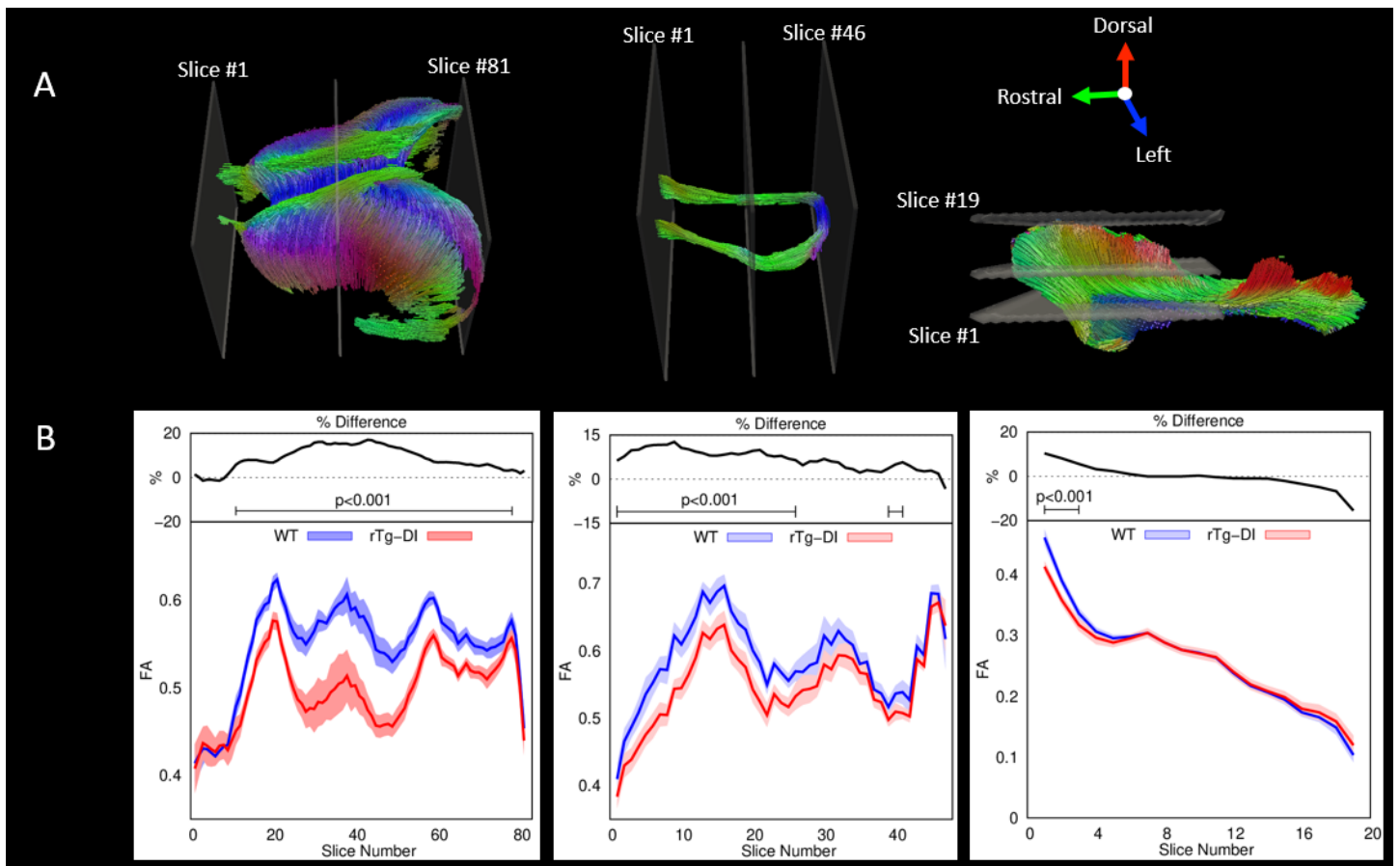
**Supplementary Figure 4: Voxel-wise GM morphometry comparison between rTg-DI and WT rats documented *in vivo***

The proton density weighted (PDW) MRI acquired *in vivo* was used for quantitative assessment of GM loss. **A:** Spatially normalized population averaged GM volumetric maps of 11M old rTg-DI and WT are shown in color maps. **B:** For each age group, statistical parametric maps (color coded for p-values) were calculated, corrected for multiple comparison at FDR < 0.05, and overlaid onto the population averaged PDW MRI images to display anatomical areas. Anatomical levels of the axially displayed anatomical templates are given by their nearest Bregma distance.



**Supplementary Figure 5: Population averaged WM volume maps documented *in vivo***

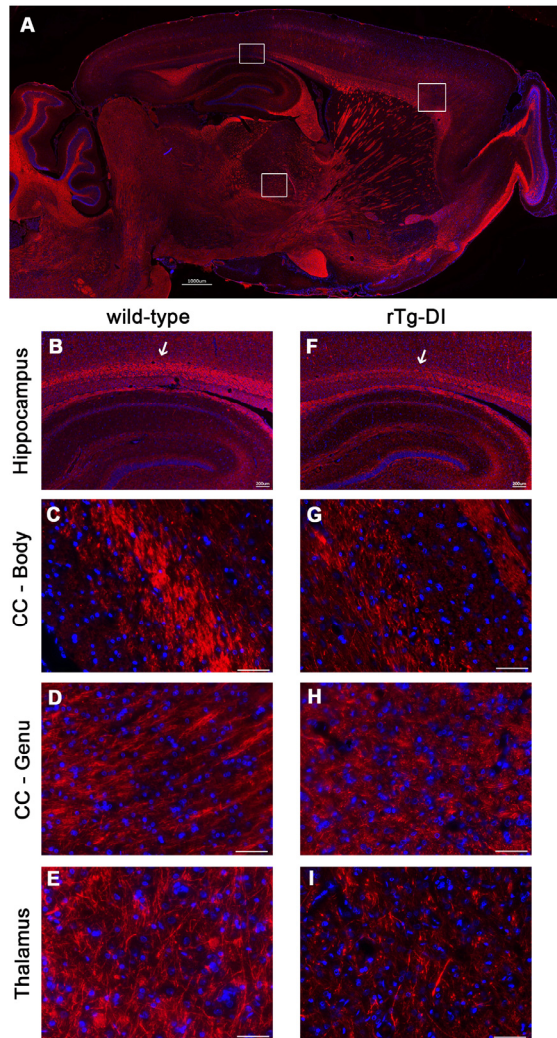
Population averaged whole brain WM volumetric maps of WT (N=11) and rTg-DI (N=11) at 3M, 6M, 9M and 11M of age are shown. For each animal, a deformation field derived from the DARTEL spatial registration was applied onto a WM segmented image in native space for spatial normalization. Spatially normalized WM maps were further modulated by Jacobian determinant to preserve the total brain volume and population averaged.



**Supplementary Figure 6: DTI based tractography of WM tract differences between WT and rTg-DI strains**

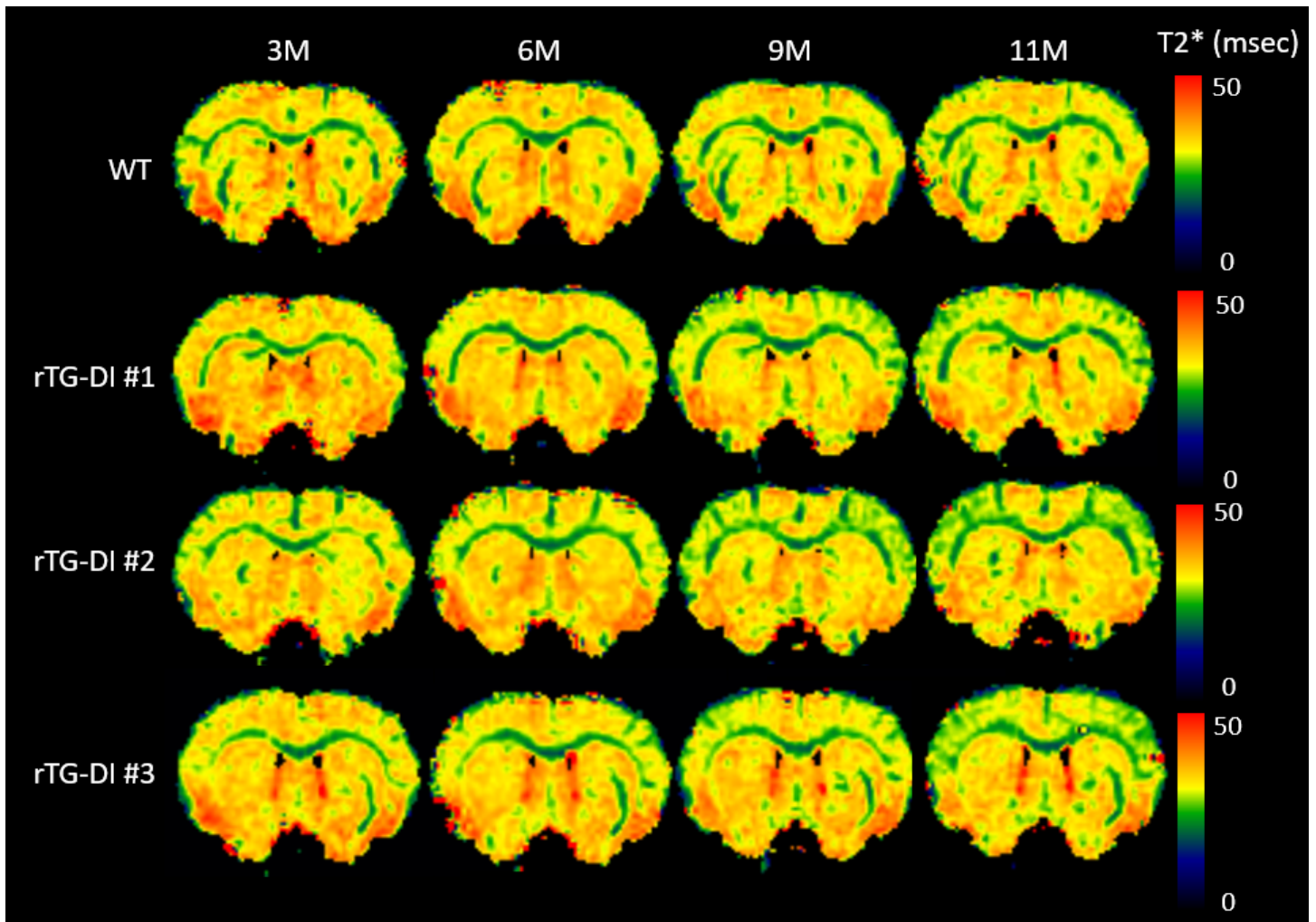
**A:** Direction encoded tractography in the corpus callosum (CC) (left), anterior commissure (AC) (middle), and projection fibers from corpus callosum to frontal cortex (FC) (right) are shown. Arrows indicate the direction of color encoded tracts. Rectangular panels represent image planes used for calculating 2D FA slice profiles in each structure. **B:** Mean (solid lines) and standard deviation (SD) (shaded) of FAs within each slice are plotted as a function of slice. % differences (solid white lines) between rTg-DI and WT rats in each slice were plotted above the FA slice profile. Significant differences between the two groups revealed by t-test were shown in solid lines below the percent differences ( $p$ -value  $< 0.001$ ).





### Supplementary Figure 7: Axonal loss and fragmentation in rTg-DI rats validated by histology

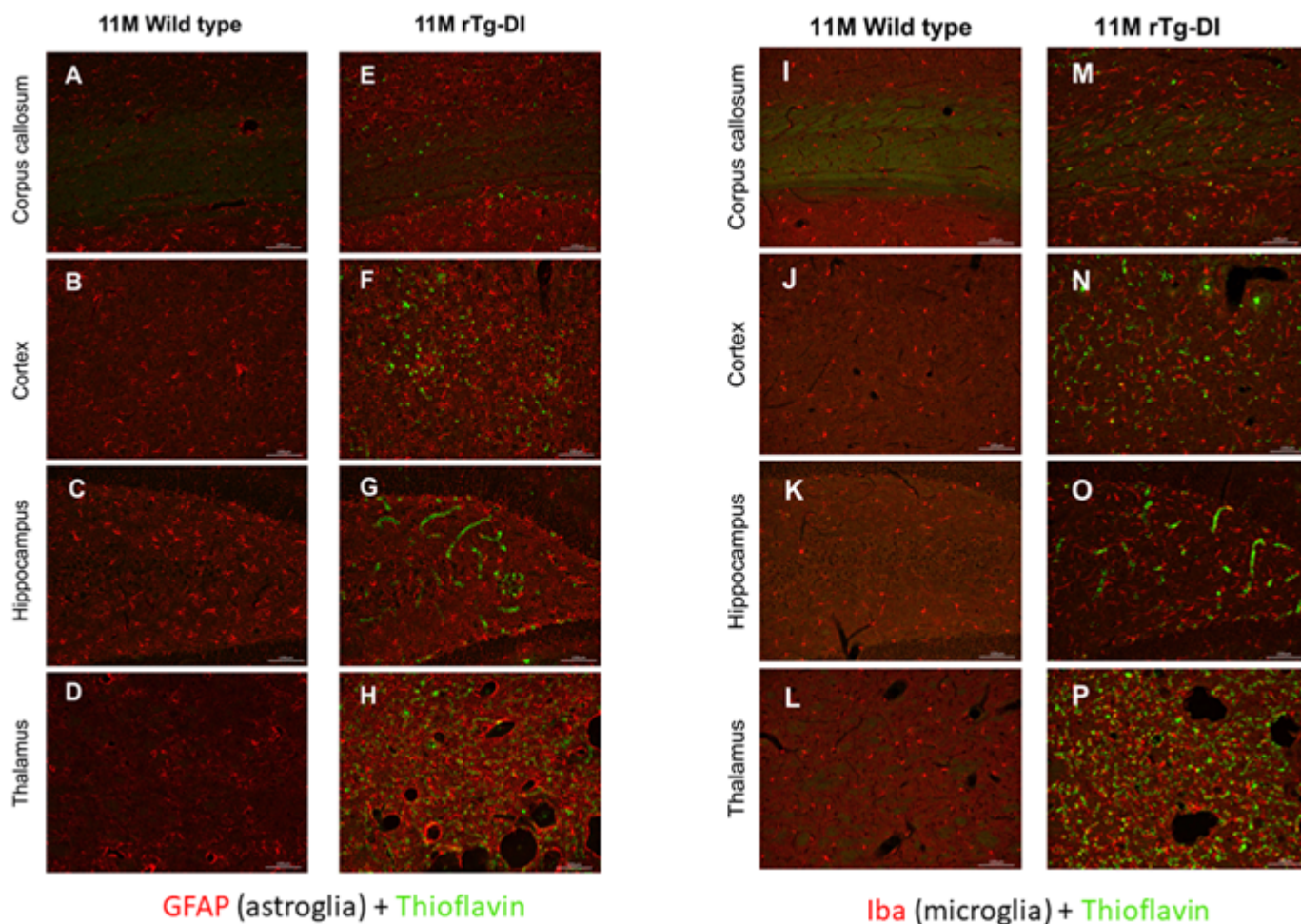
A: Representative sagittal section from a 11 month (M) old rTg-DI rat immunolabeled for axons using the pan-axonal neurofilament marker SM312 and DAPI. The three white boxes highlight the anatomical locations presented in the panels below: Corpus callosum (CC) body above the dorsal hippocampus, CC-Genu and the thalamus. The left panel set shows representative images of the dorsal hippocampus and the three preselected regions from a 11M old WT rat (B-E) and an 11M old rTg-DI rat (F-I). Thinning of the body of the CC above the dorsal hippocampus is noted in the 11M rTg-DI rat (F arrow, G) compared to the 11M WT (B arrow, C). Decreased labeling of axons signifying general axonal loss was evident throughout the CC of the 11M rTg-DI rat (G). At the level of the genu, disruption of the axonal labeling is evident and the axonal segments appear fragmented in the rTg-DI rat (H) compared to the WT rat (D). In the thalamus, labeling of axons is strikingly reduced in the 11M rTg-DI rat (I) compared to WT (E). (A) scale bar = 1000  $\mu\text{m}$ ; (B, F) scale bars = 200  $\mu\text{m}$ ; (C-E) and (G-I) scale bars = 50  $\mu\text{m}$ .



**Supplementary Figure 8: T2\* hypointensity in cortices documented *in vivo***

Representative spatially normalized T2\* map of one WT rat and three rTg-DI rats at 3M, 6M, 9M and 11M of age are displayed axially at 0.48 mm Bregma distance. In WT, T2\* maps appear similar and reproducible across all time points. Three cases of rTg-DI rats indicate the T2\* hypo-intensities in cortex, which appear as diffuse or columns, emerged at 9M which then progressively became more conspicuous over time.





### Supplementary Figure 9: Perivascular neuroinflammation in 11M rTg-DI rats

Pronounced perivascular neuroinflammation in 11M rTg-DI rats (E-H and M-P) compared to WT rats (A-D and I-L) was evident in the form of astrogliosis (GFAP in red) and activated microglia (Iba-1 in red) in regions with heavy perivascular fibrillar A $\beta$  burden (green) such as the thalamus and hippocampus in comparison to WT.

Scale bars = 100  $\mu$ m.